Third International Symposium on Marine Propulsors
smp'13, Launceston, Tasmania, Australia, May 2013

An Automatic Optimization Process for Optimal Ducted Propeller Design and Its Application Based on CFD Techniques*

Long Yu[1], Markus Druckenbrod[2], Martin Greve[2], Moustafa Abdel-Maksoud[2]

[1]School of Naval Architecture and Ocean Engineering, Shanghai Jiao Tong University, China
[2]Institute of Fluid Dynamics and Ship Theory, Hamburg University of Technology, Germany

ABSTRACT

An optimization design method is provided for ducted propeller steady analysis. It combines geometry generation, auto-meshing, optimization algorithm and CFD analysis techniques and make the process automatic operated which helps extend the CFD analysis to the design process. For test the whole process, a ducted propeller case study is validated and optimized, which is a propeller substitution and upgrading for higher thrust force and efficiency. The optimum result can provide better thrust force than original ducted propeller installed on the vessel. Some necessary techniques are studied for make the process smoothly operated.

Keywords

panel method, RANSE solver, automatic optimization process

1 INTRODUCTION

A Ducted Propeller typically consists of a rotor, a nozzle and a hub. Optimization of ducted propellers is of a long history topic while many researchers devoted their minds on it. Some of them are focus on studying fundamental geometry parameters like Yoshishisa T et al.(2005) while some focus on developing new optimization algorithms such as Naujoks B et al.(2007). To theoretically analyze the phenomenon of ducted propeller methods based on two kinds of methods. One is Boundary Element Method(BEM), which is proved to be promising in predicting performance of ducted propulsions. Kerwin et al. (1987) gave a first systematic view of inviscid flow fields around a ducted propeller and discussed panel arrangements and gap influences on the tip vortices. Hughes (1997) and Baltazar et al. (2009) continued the analysis of ducted propeller from wake analysis and tip gap flow. Gu and Kinnas(2003) modeled the flow around a ducted propeller by a vortex lattice and finite volume methods. Moon et al. (2002) extended panel method to investigate a multi-component propulsor. The other is Reynolds Average Navier-Stokes Equations (RANSE) , which is also introduced to investigate ducted propellers such as Abdel-Maksoud et al. (1999) (2002) and Haimov (2010). RANSE code can predict the performance of ducted propellers quite well but it is also time consuming and has much difficulty at geometry modeling and meshing. These are obstacles for optimization design.

A series work based on both potential method and RANSE solver for the whole geometry have been done for a multi-component linear jet optimization by Abdel-Maksoud et al.(2010) and Steden M et al.(2009).

Based on these previous work, this paper investigates open water performance computation efficiency by introducing a new fast geometry modeling and meshing program for both potential and RANSE solvers. Based on this, an optimization process can be built to make the RANSE solution automatically fulfilled. A first order panel method is applied to predict the hydrodynamic characteristics of the ducted propeller at the preliminary analysis. Then, the RANSE code is used at final design stage. A numerical computation for a propeller upgrading case is fulfilled by this design process for validation.

2 THEORETICAL BACKGROUND

2.1 Boundary Element Method

When applying a BEM, only the geometric boundaries of the propeller, the hub and the duct are discretized. The direct panel method—panMARE (2011) is the in-house code of the Institute of Fluid Dynamics and Ship Theory (FDS) at the Hamburg University of Technology (TUHH). It is based on a solution of Laplace's equation $\Delta\Phi^* = 0$, where Φ^* is the total velocity potential consisting of the free stream potential Φ_∞ and the perturbation potential Φ . The general solution for the perturbation potential on a surface boundary reads:

$$\Phi(x) = \frac{1}{4\pi}\int_{S_B} \mu \frac{\partial}{\partial n}\left(\frac{1}{r}\right) dS - \frac{1}{4\pi}\int_{S_B} \sigma\left(\frac{1}{r}\right) dS \qquad (1)$$

using the dipole strength $-\mu = \Phi$ and the source strength

*

$-\sigma = \partial\Phi/\partial n$. The potential is solved using a linear combination of sources and doublets for the discretized geometry superimposed with the inflow velocity(Abdel-Maksoud et al.(2010)).

The strength of the trailing vortices is found by the linear Kutta condition defined at the trailing edge:

$$\mu_{wake} = \mu_{upper} - \mu_{lower} \quad (2)$$

Additionally, an empirical friction-correction formulation is implemented to account for viscous effects. The shape of the trailing wake surfaces can be adapted to align with the local total velocity vector.

2.2 RANSE solver

RANSE calculations are performed by the commercially available numerical code ANSYS-CFX, which is based on Finite Volume Method. It absorbed accuracy of Finite Element method while conservation is kept. It interpolates using 24 nodes for hexahedral elements much more accurate than traditional FVM which using only 6 nodes.

Multi Reference Frame(MRF) technique is applied for simulation of the flow behavior in rotating domains. As shown in Figure 1, general Grid Interfaces (GGI) boundary condition is applied at the subdomain interfaces. This boundary condition allows matching numerical grids with different resolutions.

Figure 1 Computation Model with Periodical Conditions for RANSE Solution

In the computation, undisturbed velocity as an inlet boundary condition and pressure outlet condition are used. The periodic interfaces are applied for reduction the computation time. Only one quarter model has been analyzed.

3 GEOMETRY GENERATION AND MESHING

3.1 Geometry generation

A computer program, named Caly, is developed to

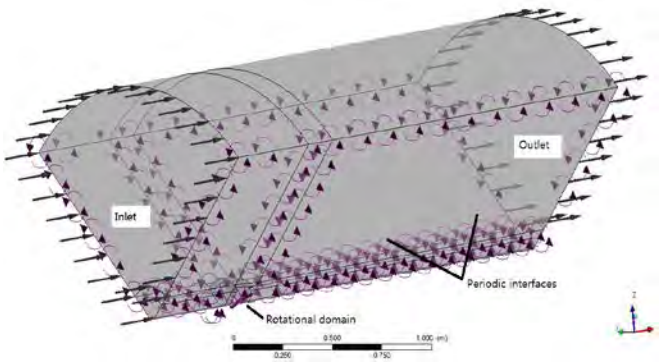

generate the geometry of blade, duct and hub while surface panels are created simultaneously. The initial wake shape of the blade aligns with the pitch of each cylindrical section of the propeller blade. The applied Cartesian coordinate system (x, y, z) shown in Figure 2, where the blade rotates in a clockwise direction (front view). The ship moves toward the $-x$ direction. The propeller is a controllable pitch propeller.

Figure 2 Geometry and coordinate of a ducted propeller

3.2 Auto-meshing

Different from the interactive way of generating a structured grid, Caly, combined with ANSYS-TurboGrid package, allows a drastic reduction in the computational time needed for the geometry and grid generation process. The block topology for O or C grid is depicted with control points.

In order to create high-quality structured finite volume grids for the propeller domain, ANSYS-TurboGrid package is introduced for meshing the blade and part of the duct domain. It allows generating high-quality hexahedral meshes for rotating machinery, which can be used to solve complex blade passage problems. The package includes an Automatic Topology and Meshing (ATM Optimized) feature, which enables improving the quality of the numerical meshes without having to make manual control point adjustments.

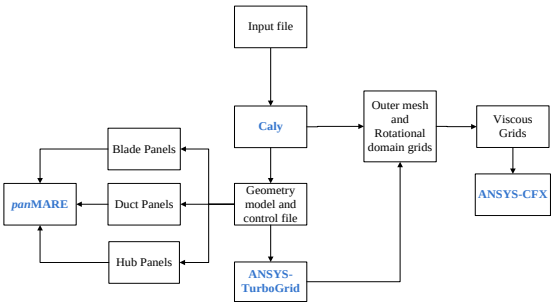

Figure 3 Workflow of Caly

The workflow of Caly is shown in Figure 3, while grid generation for the RANSE code is carried out in three steps. In the first step, Caly generates all the geometry including particular control files for ANSYS-TurboGrid. Then it generates the grids for the whole region except the propeller domain. In this step, different topologies of the duct domain grid can be applied, after that Caly generates the control parameters for interaction with the ANSYS-

TurboGrid to meshing rotational domain. Finally, both meshes are combined into one by script. In general, simply meshing the ducted propeller domain using the conventional method requires at least several hours for an experienced person. However, the method developed in this study reduces computational time to less than an hour.

The dimension of computation domain is divided into 10 blocks. Suppose D is the diameter, inflow block length is 4D, height is 4D, the middle block is controlled by duct height. The propeller domain length is D, the slipstream domain is 10D.

4 AUTOMATIC OPTIMIZATION PROCESS

The automatic optimization process is shown in Figure 4.

An evolution algorithm—MAES, based on meta-model(Abdel-Maksoud et al.(2010)), is used as gross control of the process. An object function is developed for calculate a minimum linear combination of efficiency, thrust force and possibility of cavitation by counting the low pressure level of total grids.

For one iteration, firstly, Caly builds three dimensional models for blade, hub and nozzle and generates grids for panel methods. Then it governs ANSYS software package to generate hexahedral grids and forms computation model. Secondly, panMARE is used for preliminary design to narrow the bounds for the design variables due to its fast computation ability(left rectangle in Figure 4). Finally, Ansys.CFX is employed for fine optimization results(right rectangle in Figure 4).

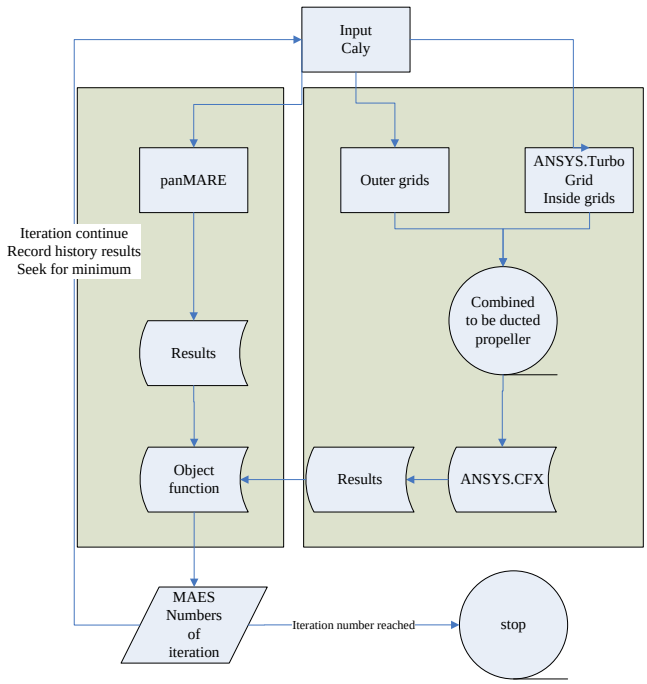

Figure 4 Outline of optimization process

5 SOME KEY TECHNIQUES

5.1 Negative volume

Automatic meshing by Ansys.TurboGrid may produce negative volume due to the arbitrary geometry. A mesh file is generated to record the minimum volume. If it is negative value, the process will ignore the step and regenerate the input values and loop again.

5.2 Object function

The purpose of optimization process is to seek for an optimum propeller. There are many goals can be used as object while three of them are chosen as the main factors, they are thrust coefficient, efficiency and cavitation possibility. A linear combination of these objectives is used to transfer a multi-criteria object to be single object.

5.2.1 Thrust coefficient

Maximize the thrust force is one of the main purpose, so thrust coefficient of the whole ducted propeller—Ktt is used to represent this request.

$$K_{tt} = \frac{F}{\rho n^2 D^4} \tag{3}$$

Where n is the rotation speed, D is diameter of the propeller. F is the total thrust force.

5.2.2 Efficiency

The efficiency of the ducted propeller is most important object, which defined as:

$$\eta = \frac{JK_{tt}}{2\pi K_Q} \tag{4}$$

Where J is advanced coefficient, K_Q is the torque coefficient.

5.2.3 Cavitation possibility

The cavitation is measured by cavitation number, defined as:

$$\sigma = \frac{P_0 - P_v}{\frac{1}{2}\rho V^2} \tag{5}$$

Where P_0 is the reference pressure taken at a given point, P_v is standard vapor pressure, V is propeller advance velocity.

The cavitation phenomenon indexed with possibility of occurrence. Pressure of each element has been calculated and compared with standard pressure which represents initiation of cavitation. If the pressure of element is lower than standard vapor pressure, then it is recorded as occurrence of cavitation. The division of numbers of these elements and total elements numbers is the cavitation possibility.

6 CASE STUDY

For an upgrading of propulsion system for a dredger, which is a heavy load vessel at low speed, the main design parameters are listed in table1. According to the test carried out at model basin, a ducted propeller has been proved and installed as an optimum solution for the upgrading as Figure 2. However, by the automatic design process, further optimization can be fulfilled. Model size has been used because it is convenient to compare with experiment data directly.

Table 1 Basic parameters

Items	Value
Diameter of propeller (D)	200 mm
Number of blades	4
Duct length (D_n)	100 mm
Hub diameter (D_h)	48 mm
Rotational speed (n)	3.59 rev/s

6.1 Experiment data

For comparison, an experiment data for the case is introduced for verification. The geometry of the ducted propeller is shown in Figure 2. The open water performance curves are shown in below. The experiment data are represented by dots while continued lines represent calculation results by ANSYS.CFX.

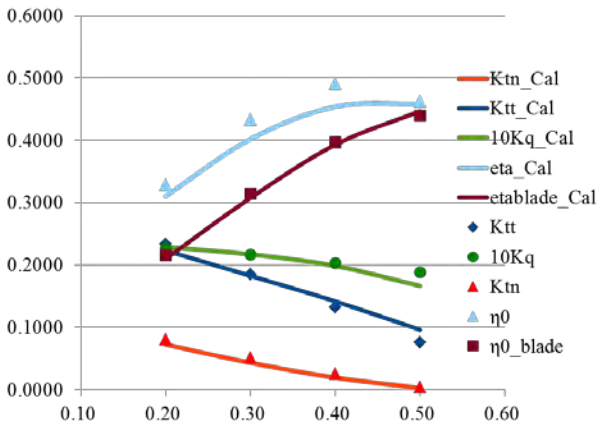

Figure 5 Validation computation

6.2 Potential optimization process and results

For simplicity, the duct is determined to be 19A. The original blade is described by 3 section files. The pitch, chord length, distance to leading edge and maximum thickness are chosen to be design variables. Potential solver—panMARE is used for preliminary design and narrow the design variable boundary.

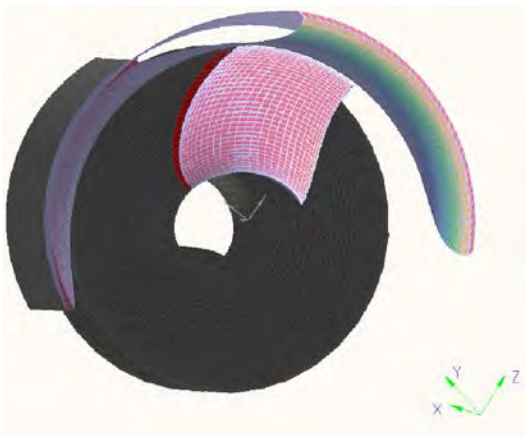

Figure 6 One quarter model calculated with periodic boundary conditions

Table 2 Design variables

Design variables	Preliminary		Fine		Optimum
	Lower Bound	Upper Bound	Lower Bound	Upper Bound	
P1	0.6	1.0	0.7	0.9	0.896
P2	0.6	1.0	0.85	0.9	0.899
P3	0.6	1.0	0.5	0.9	0.644
C1	2	12	3	10	3.394
C2	2	12	6	10	8.829
C3	2	12	4	10	5.752
D1	0	10	0	8	5.131
D2	0	10	0	6	5.547
D3	-3	5	-1	1	0.428
M1	1	6	3	4	3.049
M2	1	6	1.5	3.5	2.372
M3	1	3	0.1	0.3	0.253

7 CONCLUSION

After 1000 steps for optimization, the minimum object has been found, as shown in Figure 7.

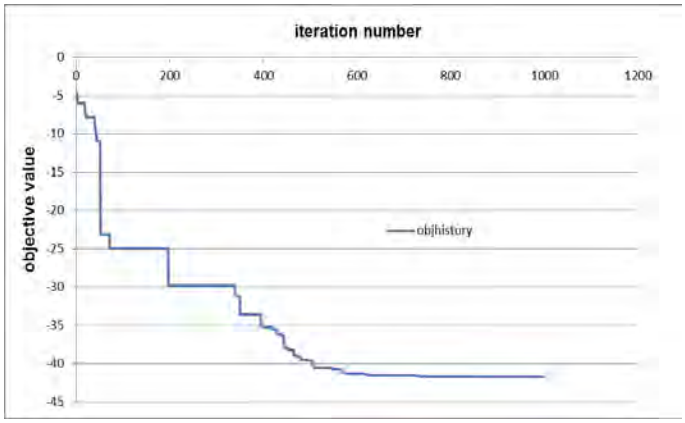

Figure 7 Optimization process

The geometry of optimized propeller is shown as Figure 8.

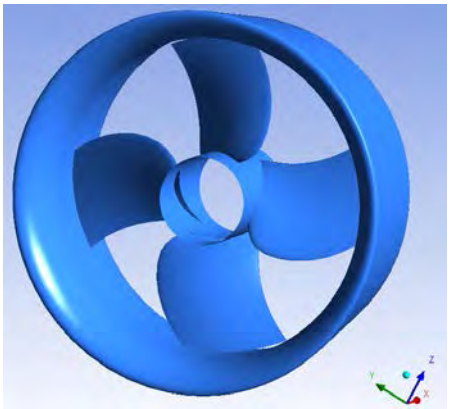

Figure 8 Optimized geometry of ducted propeller

The optimization design can provide bigger thrust force and less cavitation occurrence with much higher efficiency especially at low speed(Table 3). Installed refers to original ducted propeller while optimized refers to optimum one.

Table 3 Optimization improvement

J	item	K_{tt}	K_Q	efficiency
0.20	installed	0.2232	0.2289	0.3104
0.30		0.1826	0.2170	0.4018
0.40		0.1416	0.1986	0.4541
0.50		0.0959	0.1663	0.4588
0.20	optimized	0.2898	0.2765	0.3336
0.30		0.2431	0.2641	0.4394
0.40		0.1964	0.2443	0.5118
0.50		0.1158	0.1972	0.4674
0.20	(Optimized-Installed)/Optimized	22.98%	17.22%	6.96%
0.30		24.87%	17.85%	8.54%
0.40		27.87%	18.70%	11.28%
0.50		17.20%	15.65%	1.84%

From Figure 9, pressure inside optimized propeller duct is higher than the original one, which represents bigger nozzle thrust force achieved.

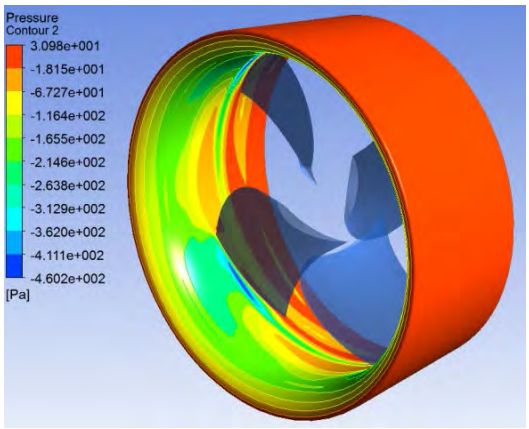

(a) optimized

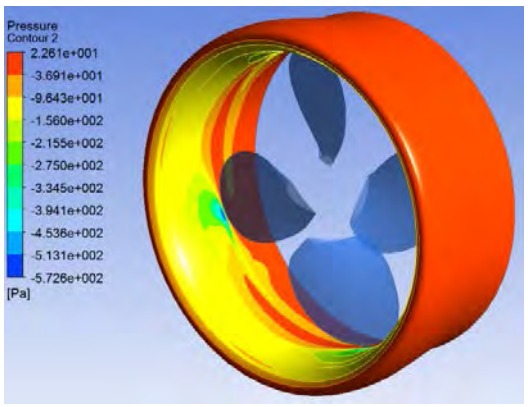

(b) installed

Figure 9 Contour of duct pressure distribution for both propellers

The automatic optimization process is also time-consuming and very sensitive to the geometry twisting so that only the blade is chosen for optimization and one successfully fulfilled round has been shown. The bounds of design variables should be proper determined by potential solver in preliminary process. The duct and hub geometry generating and changing will be the further research topic. The strength consideration in this process should also be considered in the next research work.

8 ACKNOWLEDGEMENT

The author thanks the China Scholarship Council (CSC) and National Natural Science Foundation of China(No:51009090) for their support. Special thanks to Prof. Dr.-Ing. Moustafa Abdel-Maksoud for kindly guidance and valuable suggestions. Thanks also give to Dipl.-Ing. Martin Greve and Dipl.-Ing. Markus Druckenbrod for their help and cooperation.

REFERENCES

Abdel-Maksoud M and Heinke H-J (1999) Investigation of viscous flow around modern propulsion systems. In: Proceedings of CFD'99. Ulsteinvik, Norway

Abdel-Maksoud M and Heinke H-J (2002) Scale Effects on Ducted Propellers. In: Proceedings of the 24th Symposium on Naval Hydrodynamics, Fukuoka, Japan, pp 744-759

Abdel-Maksoud M, Steden M and Hundemer J (2010), Design of a Multi-Component Propulsor. In: Proceedings of 28th Symposium on Naval Hydrodynamics, Pasadena, USA, September

Baltazar J and Falcão de Campos, Bosschers J (2011) Open-Water Thrust and Torque Predictions of a Ducted Propeller System with a Panel Method. In: Proceedings of the Second International Symposium on Marine Propulsors, Hamburg, Germany, pp 132-141

Gu H and Kinnas S A (2003) Modeling of contra-rotating and ducted propellers via coupling of a vortex-lattice with a finite volume method. In: Proceedings of Propeller/Shafting 2003 Symposium, SNAME, Virginia Beach, U.S.A.

Haimov H, Bobo M J, Vicario J and Corral J del (2010) Ducted Propellers. A Solution for Better Propulsion of Ships Calculations and Practice. In: Proceedings of 1st International Symposium on Fishing Vessel Energy Efficiency E-Fishing, Vigo, Spain

Hughes M J (1993) Analysis of Multi-Component Ducted Propellers in Unsteady Flow. Ph.D Thesis, Department of Ocean Engineering, MIT

Kerwin, J. E., Kinnas, S. A., Lee, J.-T. & Shih, W.-Z. (1987). 'A surface panel method for the hydrodynamic

analysis of ducted propellers', Transactions of Society of Naval Architects & Marine Engineers **95**.

Moon Il-S, Kim K S and Lee C S (2002), Blade Tip Gap Flow Model for Performance Analysis of Waterjet Propulsors. In: Proceedings of International Association for Boundary Element Methods. UT Austin, TX, USA.May 28-30

Naujoks B, Steden M, Mueller S-B, and Hundemer J (2007), Evolutionary Optimization of Ship Propulsion Systems, IEEE Congress on Evolutionary Computation(CEC 2007),2809-2816

panMARE (2011), Institute of Fluid Dynamics and Ship Theory, Hamburg University of Technology, www.panmare.de

Steden M, Hundemer J, Abdel-Maksoud, M(2009), Optimisation of a linearjet, First International Symposium on Marine Propulsors, Trondheim, Norway.

Yoshishisa T, Takafumi K, Hajime Y et al.(2005), Study on the design of propeller blade sections using the optimization algorithm, Journal of Marine Science and Technology, 70-81